Available online at www.sciencedirect.com
SCIENCE DIRECT®
International Journal of Thermal Sciences 43 (2004) 761–767
International Journal of Thermal Sciences
www.elsevier.com/locate/ijts

Transient flow and heat transfer phenomena in inclined wavy films

Katerina Serifi [a], Nikolaos A. Malamataris [b], Vasilis Bontozoglou [a,*]

[a] *Department of Mechanical and Industrial Engineering, University of Thessaly, 38334 Volos, Greece*
[b] *Department of Mechanical Engineering, Technological Educational Institution of Western Macedonia, 50100 Kila Kozani, Greece*

Received 20 August 2003; received in revised form 18 December 2003; accepted 24 February 2004

Available online 28 May 2004

Abstract

A finite-element numerical scheme is used to study rigorously the flow of an inclined liquid film and the heat transfer from the constant-temperature wall. Regular inlet disturbances are predicted to evolve into periodic or solitary waves depending on the frequency of the forcing. At very low disturbance frequencies parasitic crests appear and the regularity of the wavetrain is lost. The effect of a solitary wavetrain on heat transfer from the wall is studied, and it is predicted that a stationary temperature distribution develops with periodic flux variation that follows the waves. The thinning of the substrate between successive humps combines with the effect of convection at the crest and tail of the solitary humps to produce heat transfer enhancement significantly above the conduction limit.

Keywords: Film flow; Solitary waves; Wall heat transfer; Enhancement; Finite-element

1. Introduction

Film flow occurs in a variety of process equipment, including condensers, falling film evaporators, absorption columns and two-phase flow reactors. In a range of Reynolds numbers of interest to such engineering applications ($1 < Re < 400$) the flat free surface is unstable and traveling waves develop. These surface waves have long been known to affect heat and mass transfer across the film [1]. However, the flow problem is extremely complex because the location of the free surface varies continuously and must be found as part of the solution. Consequently, efforts to explain the influence of waves on transport processes have to some extent relied on heuristic modeling [2–5], and only few studies have adopted rigorous numerical solution of the flow and energy transport equations [6–9].

Of particular interest among the various wave forms adopted by the free surface are solitary waves, ie. strongly nonlinear humps proceeded by capillary ripples, which attain a stationary shape and are separated by relatively long stretches of flat substrate. It has been observed [10] that in many circumstances the downstream evolution of film flow tends to a series of solitary waves. This occurs directly when regular disturbances of low frequency are introduced at the inlet, and indirectly (through a sequence of nonlinear interactions) when the inlet disturbance consists of random noise.

Thus, the goal of the present contribution is to investigate computationally the dynamics of the unstable free surface of an inclined liquid film, as well as its influence on heat transfer across the film. The full Navier–Stokes equation is solved by a finite-element method, delineating the evolution of the free surface and the flow field below the waves. The flow is considered from the initial stages of linear instability up to the development of stationary traveling waves [6]. The energy equation is solved subsequently with the same method, providing information on the effect of waves on heat transfer.

Emphasis is placed on the role of solitary waves, and in particular at low wall inclinations and relatively small Reynolds numbers. These conditions lead to the formation of two-dimensional free-surface waves without recirculation at the crest, whose properties and interactions have been experimentally documented [10,11]. Thus, the present study is closely related and complementary to recent work by Miyara [9], who used a finite-difference method to investigate heat transfer on a vertical film at significantly higher *Re*.

* Corresponding author.
E-mail addresses: nikolaos@eng.auth.gr (N.A. Malamataris), bont@mie.uth.gr (V. Bontozoglou).

1290-0729/$ – see front matter
doi:10.1016/j.ijthermalsci.2004.02.016

Nomenclature

A	amplitude of inlet disturbance nondimensionalized by H
Bi	Biot number, $= hH/k$
c	dimensionless phase velocity of waves nondimensionalized by U
f	disturbance frequency ..... s^{-1}
Fr	Froude number, $= U/(gH)^{1/2}$
g	gravitational constant ..... $m{\cdot}s^{-2}$
H	Nusselt film thickness ..... m
h	heat transfer coefficient ..... $W{\cdot}m^{-2}{\cdot}K^{-1}$
H_c	free surface curvature ..... m^{-1}
k	thermal conductivity ..... $W{\cdot}m^{-1}{\cdot}K^{-1}$
$\underline{n}$	unit normal vector at free surface
p	dimensionless pressure nondimensionalized by ρU^2
Pr	Prandtl number, $= \nu/\alpha$
Pe	Peclet number, $= UH/\alpha$
Q	liquid flow rate per unit span ..... $m^2{\cdot}s^{-1}$
q	heat flux ..... $W{\cdot}m^{-2}$
Re	Reynolds number, $= Q/\nu$
T	temperature ..... K
t	dimensionless time nondimensionalized by H/U
U	mean velocity of liquid ..... $m{\cdot}s^{-1}$
u	dimensionless streamwise velocity nondimensionalized by U
v	dimensionless normal velocity nondimensionalized by U
x	dimensionless streamwise distance nondimensionalized by H
y	dimensionless distance normal to the wall nondimensionalized by H
We	Weber number, $= \sigma/\rho U^2 H$

Greek symbols

α	thermal diffusivity ..... $m^2{\cdot}s^{-1}$
η	dimensionless film thickness nondimensionalized by H
θ	dimensionless temperature temperature scale $(T_w - T_a)$
μ	viscosity ..... $kg{\cdot}m^{-1}{\cdot}s^{-1}$
ν	kinematic viscosity ..... $m^2{\cdot}s^{-1}$
ρ	density ..... $kg{\cdot}m^{-3}$
σ	surface tension ..... $N{\cdot}m^{-1}$
$\underline{\underline{\tau}}$	dimensionless stress tensor nondimensionalized by ρU^2
φ	inclination angle ..... degrees
φ_i	biquadratic Galerkin basis function
ψ_i	bilinear Galerkin basis function

Subscripts

m	mean value across the film
a	conditions along the front part of wall
w	conditions along the main part of wall
i	finite-element node
s	free surface

2. Mathematical formulation and numerical solution

Two-dimensional, gravity-driven flow down a plane with inclination φ relative to the horizontal is considered, as sketched in Fig. 1. The mean volumetric flow rate per unit span is denoted by Q_m and the Re number is defined as $Re = Q_m/\nu$, where ν is the kinematic viscosity, $\nu = \mu/\rho$. Coordinate x is in the streamwise direction and coordinate y is normal to the plane. The location of the free surface and the magnitude of the instantaneous volumetric flow rate per unit span generally vary with x and t and are described by the functions $\eta(x,t)$ and $Q(x,t)$, respectively. For reference, we recall the classical Nusselt solution with a parabolic x-velocity with mean value $U = g\sin\varphi H^2/3\nu$, and a uniform film with thickness $H = (3\nu^2 Re/g\sin\varphi)^{1/3}$ (thus $Q = UH$).

In the present work we consider the hydrodynamic problem of the development of nonlinear waves along the free surface of the film, as well as the thermal problem of heat transfer from the wall to the film. With respect to the latter, the flow is considered isothermal, with temperature T_a, up to a streamwise distance $x = x_0$ from the inlet, and then the wall is heated to a constant higher temperature, T_w.

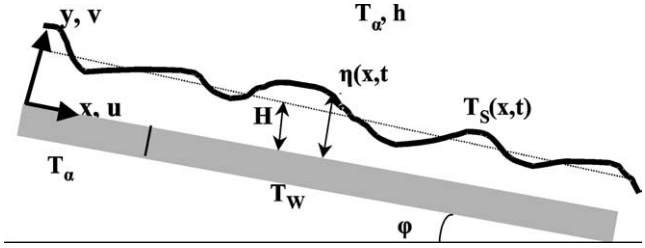

Fig. 1. Sketch of the flow system considered.

The free surface is thermally characterized by a uniform air temperature, T_a, and a constant heat transfer coefficient, h. The effect of temperature on physical properties is neglected (passive scalar transport) and thus the two problems are solved consecutively.

A complete description is provided by the continuity, Navier–Stokes and energy equations, together with a set of boundary conditions. We use U, H and $(T_w - T_a)$ as the characteristic velocity, length and temperature scales. We nondimensionalize time and pressure with the magnitudes H/U and ρU^2, respectively, and temperature with $\theta = (T - T_a)/(T_w - T_a)$. The resulting equations in dimensionless form are:

$$\underline{\nabla}\cdot\underline{u}=0 \tag{1}$$

$$\frac{\partial \underline{u}}{\partial t}+\underline{u}\cdot\underline{\nabla}\,\underline{u}=-\underline{\nabla}\,p+\frac{1}{Re}\nabla^2\underline{u}+\frac{1}{Fr^2}\underline{g} \tag{2}$$

$$\frac{\partial\theta}{\partial t}+\underline{u}\cdot\underline{\nabla}\theta=\frac{1}{Re\cdot Pr}\nabla^2\theta \tag{3}$$

Here $\underline{u}=(u,v)$ is the dimensionless velocity vector in the fluid, with u and v its components in the x- and y-direction respectively, p is the dimensionless pressure, $\underline{g}$ is the unit vector in the direction of gravity, ∇ is the gradient vector and $Fr=U/\sqrt{gH}$ is the Froude number. Because of the way the equations are nondimensionalized, the Froude number is not independent but is related to the Reynolds number by the expression $Fr^2=(Re\sin\varphi)/3$.

We further apply the no-slip and no-penetration boundary condition for the velocity along the flat wall,

$$u=v=0 \tag{4}$$

and the kinematic condition and the balance of forces along the free surface:

$$\frac{\partial\eta}{\partial t}+u\frac{\partial\eta}{\partial x}=v \tag{5}$$

$$\underline{n}\cdot\underline{\underline{\tau}}=We\,2H_c\underline{n} \tag{6}$$

The Weber number in Eq. (6) is defined as $We=\sigma/\rho U^2H$, with σ the surface tension of the fluid, $2H_c=\eta_{xx}/(1+\eta_x^2)^{3/2}$ the mean free surface curvature, $\underline{n}$ the unit vector normal to the free surface and

$$\underline{\underline{\tau}}=-p\underline{\underline{I}}+\frac{1}{Re}\left[\underline{\nabla}\,\underline{u}+(\underline{\nabla}\,\underline{u})^{\mathrm{T}}\right] \tag{7}$$

the dimensionless stress tensor of the fluid, with $\underline{\underline{I}}$ the identity matrix.

We apply the following boundary conditions at the inlet in order to introduce a small, periodic disturbance of frequency f and amplitude A in the film thickness:

$$\eta(0,t)=1+A\cos 2\pi f t \tag{8}$$

$$u(0,y,t)=\frac{3Q(0,t)}{\eta(0,t)}\left[\frac{y}{\eta(0,t)}-\frac{1}{2}\frac{y^2}{\eta^2(0,t)}\right] \tag{9}$$

Eq. (8) prescribes the oscillations of the free surface at the inlet of the computational domain and Eq. (9) imposes a parabolic velocity profile in the x-direction at the entrance. The parabolic velocity profile is expected to be an excellent approximation for the entrance conditions, given the small magnitude of the disturbances. The corresponding velocity in the y-direction is found by integration of the continuity equation, using Eq. (9) and the known dimensionless phase velocity of infinitesimal waves $c=3$. At the outflow we apply the free boundary condition in order to let the fluid leave the computational domain freely without any distortion of the flow in the interior [6].

The primary unknowns of the problem, which are the velocities u and v, the pressure p and the temperature T, along with the unknown location of the free surface η, are expanded in terms of Galerkin basis functions as:

$$u=\sum_{i=1}^{9}u_i\varphi^i,\qquad v=\sum_{i=1}^{9}v_i\varphi^i,\qquad \eta=\sum_{i=1}^{3}\eta_i\varphi^i$$

$$p=\sum_{i=1}^{4}p_i\psi^i,\qquad \theta=\sum_{i=1}^{9}\theta_i\varphi^i \tag{10}$$

where φ^i are biquadratic and ψ^i bilinear basis functions. This is a standard choice of basis functions in the application of the Gakerkin finite element method in flow problems [12].

The governing equations, weighted integrally with the basis functions, result in a set of residuals. The residuals are evaluated numerically using nine-point Gaussian integration and the resulting system of nonlinear algebraic equations is solved with the Newton–Raphson iterative method. Time integration is performed with the Crank–Nicolson scheme. Numerical accuracy has been tested by doubling the number of finite elements both in the x- and the y-direction and by reducing by half the time step. All results remain visually indistinguishable from the ones taken with higher discretization, and thus are considered mesh and time step independent.

3. Results and discussion

3.1. Development of free surface waves

Using the above computational scheme, we are able to follow the entire evolution process along the channel. The most important observation relates to the effect of the frequency of inlet forcing: More specifically, high-frequency disturbances lead to saturated periodic waves whereas low-frequency disturbances evolve directly into regularly spaced solitary waves. Relevant computational results are presented in Fig. 2(a)–(d) for $Re=19.33$, $We=5.43$ and $\varphi=6.4°$, corresponding to the conditions of the experiment of Liu and Gollub [10].

Of particular interest among the different free surface profiles are solitary wavetrains. Solitary waves are known to be the most stable of free surface patterns, and thus represent the final stage of evolution of a variety of initial conditions [13]. For example, the periodic waves of Fig. 2(a) and (b) will further downstream evolve towards an irregular series of solitary humps through subharmonic and/or sideband instabilities. As a closer scrutiny of the evolution towards a solitary hump, we present in Fig. 3 consecutive profiles of the nonlinear stage separated by 10 dimensionless time units.

As we shall see later, solitary waves have a positive influence on heat transfer from the wall even at small Re and inclination angles. Thus, it would be desirable to be able to tailor a wavetrain of the desired frequency. To this end it is interesting to note that the generation of a series of solitary pulses with very small frequency is impossible. This difficulty was reported in past experiments [10,14] and was loosely attributed to the linear instability of the extensive flat

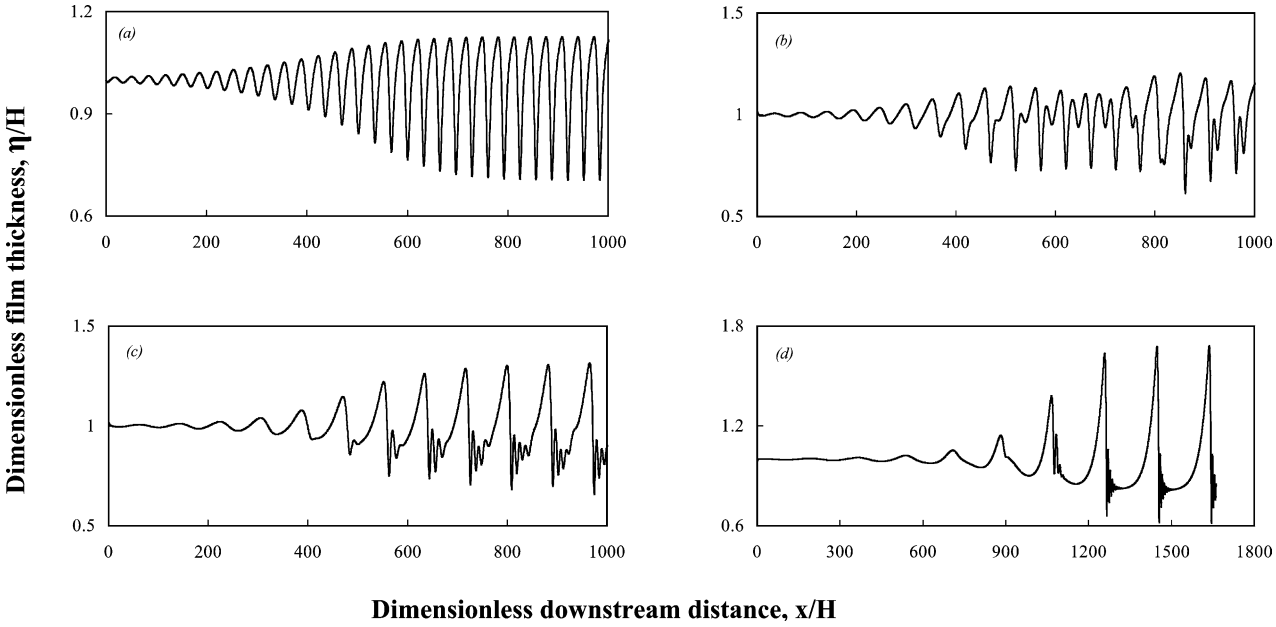

Fig. 2. Spatial evolution of the free surface for a film with $Re = 19.33$, $We = 5.43$ and inclination $\varphi = 6.4°$. The periodic inlet disturbances have frequency (a) 7 Hz, (b) 4.5 Hz, (c) 3 Hz and (d) 1.5 Hz.

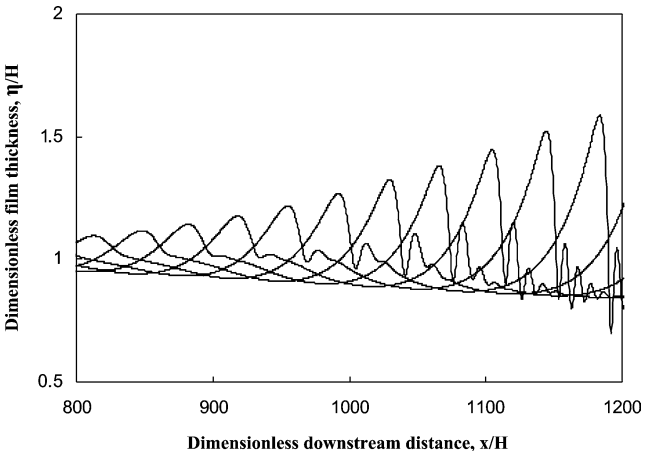

Fig. 3. The nonlinear evolution towards a solitary wave in a flow with $Re = 19.33$, $We = 5.43$ and inclination $\varphi = 6.4°$ and inlet disturbances of frequency 1.5 Hz. Curves correspond to line profiles separated by 10 dimensionless time units.

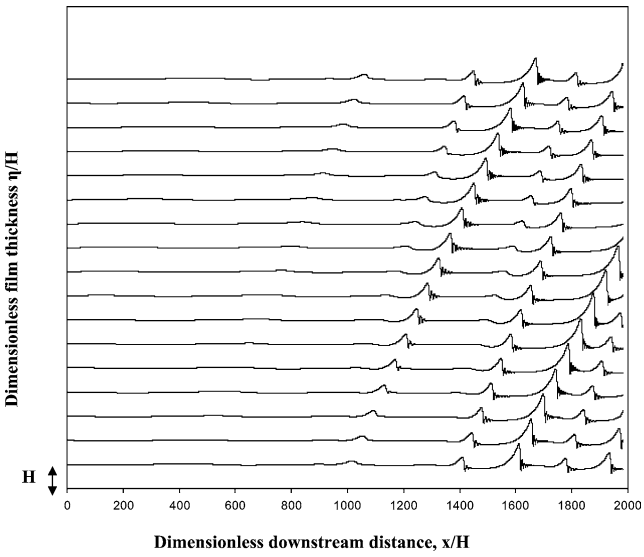

Fig. 4. Temporal evolution of the free surface for a film with $Re = 19.33$, $We = 5.43$ and inclination $\varphi = 6.4°$. The periodic inlet disturbances have a frequency of 0.5 Hz.

substrate between consecutive humps. The same observation is also born out by the present simulation and an explanation is attempted.

In particular, Fig. 4 shows time-consecutive free surface profiles for the same conditions as in Fig. 2 but with an inlet frequency of 0.5 Hz. What is observed is that parasitic crests form behind each major solitary hump. The apparent generation mechanism involves an elongated depression, which develops behind the major hump during its later stages of evolution. The back of the depression gradually steepens and a new solitary hump is formed. It is interesting to note that this process occurs in an orderly way during every cycle of the inlet forcing. Thus, it is conjectured that the phenomenon of parasitic crest generation is closely related to the radiation characteristics of the major humps. This interpretation is contrasted to the linear instability of the flat substrate that is expected to generate spatially unlocalized crests.

3.2. Effect of solitary waves on heat transfer from the wall

Next, we want to examine the effect of fully developed solitary waves on heat transfer from the wall. To this end, we consider that the system is isothermal at $T = T_a$ up to a downstream distance $x_0 = 527H$ from the inlet, and that beyond this point the wall is kept at a constant elevated

temperature T_w. The flow corresponds to the conditions of the experiment of Liu and Gollub, i.e., $Re = 19.33$, $We = 5.43$, $\varphi = 6.4°$ and $f = 1.5$ Hz. Note that the flow is created so that it has become stationary before point x_0, i.e., the solitary waves have attained a permanent shape and move with constant phase speed. In general, the downstream location where the system becomes hydrodynamically fully developed is easily modified by controlling the amplitude of inlet disturbances.

According to the nondimensionalization adopted for the temperature, $\theta_w = 1$ and $\theta_a = 0$. Also, a thermally developed flat film with thermal conductivity, k, attains a linear temperature distribution with free-surface value $T_s = (T_w + Bi\,T_a)/(1 + Bi)$ (or, equivalently $\theta_s = 1/(1 + Bi)$), where $Bi = hH/k$. The steady heat transfer through this flat thermally developed film is

$$q_0 = k\frac{(T_w - T_s)}{H} = \frac{Bi}{(1+Bi)}k\frac{(T_w - T_a)}{H} \tag{11}$$

and the value q_0 is used to nondimensionalize heat transfer through the wavy film. The problem is described in terms of the $Pe = Re\,Pr$ and Bi dimensionless numbers. The present set of results refer to constant $Re = 19.33$ and $Bi = 10$, and examine the effect of the Peclet number.

The flow conditions tested (small Re and inclination angle) do not produce waves with internal recirculation [6]. The enhancement of wall heat transfer under such conditions has previously been attributed [3] mainly to the thinning of the liquid film, which is caused by the accumulation of mass in the solitary humps. The present rigorous simulation provides a means of investigating in detail the relative effects of conduction and convection under the mild flow conditions imposed. It is recalled that vertical films at higher Re show significant enhancement, which was shown [9] to be related to the recirculating region developing under the crests.

We note at first that, though the present flow problem is fully developed, the thermal is not. If we consider the wall heat source turned on at time zero, we first have a strong temporal transient because of the very high temperature gradients close to the wall. This is a rather uninteresting facet of the problem, and we just note that the pertinent time-scale for attenuation of transient effects is governed by thermal diffusion, and thus is equal to H^2/α.

Of more interest is the spatio-temporal evolution once the initial transient has faded away, which is then only dictated by the passage of the solitary waves. Fig. 5 shows such an example, which refers to the distribution of the wall heat flux for $Pe = 50$, at two different instants separated by 20 dimensionless time units. A striking observation is that—beyond a rather short development region—a spatially periodic distribution of the heat flux appears, which is in correspondence to the instantaneous location of the solitary waves and moves with their constant phase velocity. This flux distribution indicates that the thermal problem reaches a quasi-steady state, an observation that should be expected because of the large thickness of the wall thermal boundary

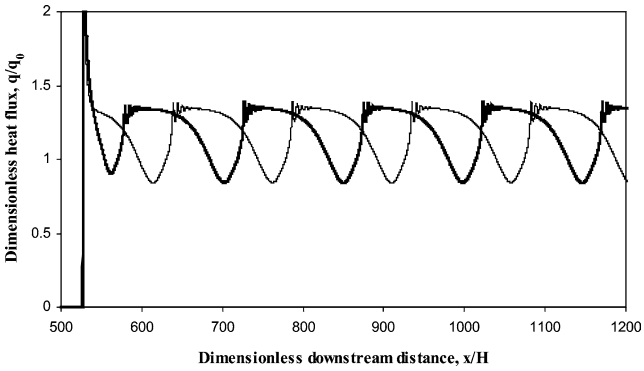

Fig. 5. The spatial distribution of wall heat flux for $Pe = 50$, at two different time instants separated by 20 dimensionless time units.

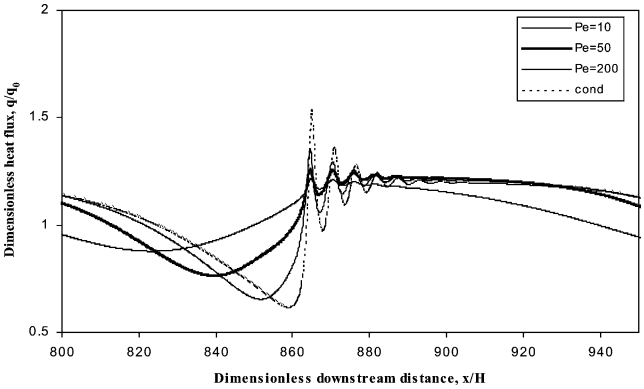

Fig. 6. The spatial distribution of wall heat flux for different Pe numbers.

layer ($Pr = 0.5$–10) compared to the thickness of the liquid film.

In order to investigate the effect of Peclet number, we consider a range of values ($Pe = 5$–200). Fig. 6 shows one period of the spatial distribution of the wall heat flux (in the quasi steady-state) for three representative cases. Also included is the hypothetical distribution, where the heat flux at each location corresponds to a thermally developed flat film (Eq. (11)) with the local thickness. The latter is considered a satisfactory approximation of the effect of pure conduction in the long-wave limit.

Fig. 6 demonstrates the effect on wall heat flux of two different time (or length) scales associated with the passage of solitary waves. The shortest scale corresponds to the oscillations of the front-running ripples. It is seen to affect heat transfer significantly less than in the conduction limit, and its net effect appears to be low. The longer scale corresponds to the wavelength of the solitary train, and it affects all the Peclet number values considered. In particular, for Peclet number < 50 the thermal behavior of the thin substrate between crests is roughly equivalent to pure conduction. These predictions can be explained by considering that the passage of each wave temporarily forces fluid parcels to approach the wall, while at the same time decelerates and elongates them in the streamwise direction. The extent of additional transient conduction

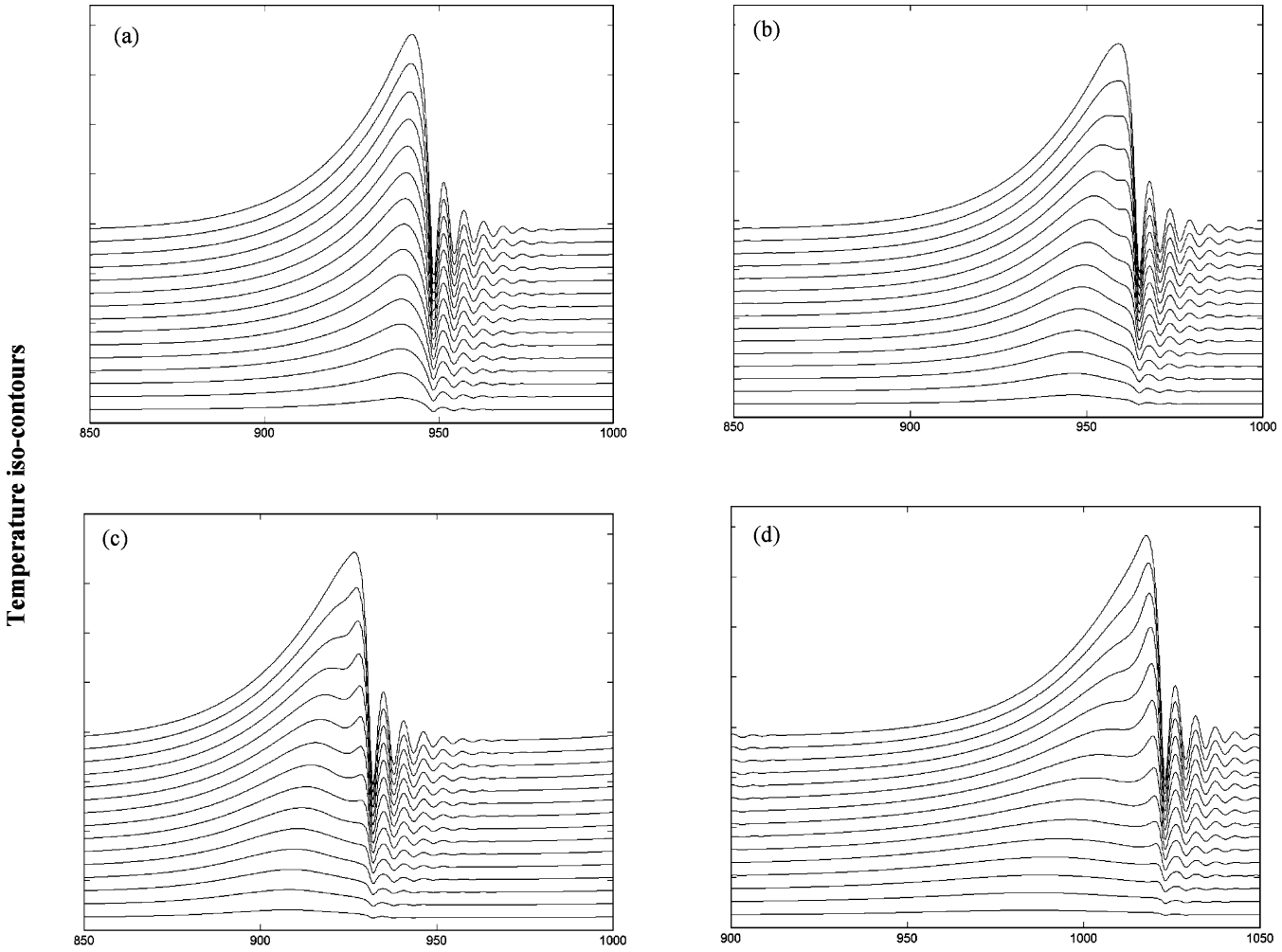

Fig. 7. Quasi-steady temperature distribution below the wave for different *Pe* numbers. (a) $Pe = 5$, (b) $Pe = 25$, (c) $Pe = 50$, and (d) $Pe = 200$.

taking place under these conditions is evidently dictated by the relation of the characteristic thermal diffusion time to the aforementioned flow oscillation scales.

In addition to the above, Fig. 6 demonstrates a nonlinear phenomenon associated with the crest of the waves. In the conduction limit, the crest offers the highest resistance to heat transfer, and thus mitigates the positive effect of the thin substrate. However, we presently observe that, with increasing Peclet number, the minimum of the wall heat flux is raised significantly and is also shifted behind the wave crest. This behavior is associated with the thermal inertia of the fluid masses transported by the solitary humps and is also manifested in the temperature field below the wave, which is depicted in Fig. 7(a)–(d). More specifically, the temperature iso-contours—which at small Peclet number are roughly self-similar to the shape of the free surface—gradually become convection-dominated, with a sharp peak at the front of the solitary hump and a weak maximum under the tail.

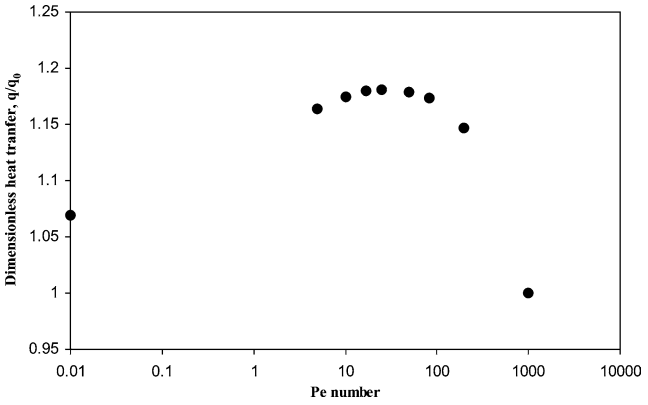

Fig. 8. The mean wall heat flux along one wavelength as a function of *Pe* number.

The mean heat flux through the wall (resulting from a combination of all the above contributions) is shown as a function of Peclet number in Fig. 8. The value for Peclet number 0.01 corresponds to the conduction limit of

Fig. 6. It is interesting to note that a significant enhancement beyond the conduction limit is predicted for a wide range of Peclet numbers. Thus, the present computation supports the conclusion that convection contributes significantly to the wall heat transfer even when the solitary waves do not have a strong recirculation.

4. Conclusions

A Galerkin finite-element scheme is used to study rigorously the flow of an inclined liquid film and the heat transfer from the wall. High-frequency inlet disturbances are predicted to evolve into saturated periodic waves and low-frequency disturbances into a wavetrain of solitary humps. Below a certain frequency parasitic crests appear and the regularity of the wavetrain is lost.

The effect of a regular solitary wavetrain on heat transfer from the wall is considered, and it is predicted that a stationary periodic flux distribution develops that follows the waves. The effect of Peclet number is studied in order to understand the relative contributions of conduction and convection to the variation of wall heat transfer. For a range of Peclet numbers, convection is found to have a significant influence at the crest and tail of the solitary humps. This effect, in combination with the thinning of the substrate between successive waves, results in heat transfer enhancement above the conduction limit.

Acknowledgements

This work was supported by the EU and the Greek General Secretariat for Research and Technology through programs PENED (01-EΔ568).

References

[1] A.E. Dukler, The role of waves in two-phase flow: Some new understanding, 1976 Award Lecture, Chem. Engrg. Educ. 11 (1977) 108–138.

[2] N. Brauner, D.M. Maron, Characteristics of inclined thin films, waviness and the associated mass transfer, Internat. J. Heat Mass Transfer 25 (1982) 99–110.

[3] S. Jayanti, G.F. Hewitt, Hydrodynamics and heat transfer of wavy thin film flow, Internat. J. Heat Mass Transfer 40 (1997) 179–190.

[4] V. Bontozoglou, A numerical study of interfacial transport to a gas-sheared wavy liquid, Internat. J. Heat Mass Transfer 41 (1998) 2297–2305.

[5] R.M. Roberts, H.-C. Chang, Wave-enhanced interfacial transfer, Chem. Engrg. Sci. 55 (2000) 1127–1141.

[6] N. Malamataris, M. Vlachogiannis, V. Bontozoglou, Solitary waves on inclined films: Flow structure and binary interactions, Phys. Fluids 14 (2002) 1082–1094.

[7] B. Ramaswamy, S. Chippada, S.W. Joo, A full-scale numerical study of interfacial instabilities in thin-film flows, J. Fluid Mech. 325 (1996) 163–194.

[8] E. Stuhltrager, A. Miyara, H. Uehara, Flow dynamics and heat transfer of a condensate film on a vertical wall—II. Flow dynamics and heat transfer, Internat. J. Heat Mass Transfer 38 (1995) 2715–2722.

[9] A. Miyara, Numerical analysis of flow dynamics and heat transfer of falling liquid films with interfacial waves, Heat Mass Transfer 35 (1999) 298–306.

[10] J. Liu, J.P. Gollub, Solitary wave dynamics of film flows, Phys. Fluids 6 (1994) 1702–1711.

[11] M. Vlachogiannis, V. Bontozoglou, Observations of solitary wave dynamics of film flows, J. Fluid Mech. 435 (2001) 191–215.

[12] P.M. Gresho, R.L. Sani, Incompressible Flow and the Finite Element Method, Wiley, New York, 1998.

[13] H.-C. Chang, E.A. Demekhin, E. Kalaidin, Secondary and tertiary excitation of three-dimensional patterns on a falling film, J. Fluid Mech. 270 (1994) 251–275.

[14] S.V. Alekseenko, V.Y. Nakoryakov, B.G. Pokusaev, Wave formation on a vertical falling liquid film, AIChE J. 31 (1985) 1446–1460.